Sub-Electron noise measurements on RNDR Devices

Stefan Wölfel, Sven Herrmann, Peter Lechner, Gerhard Lutz, Matteo Porro, *Member, IEEE*, Rainer Richter, Lothar Strüder, Johannes Treis

***Abstract*— In this work we demonstrate theoretically and experimentally the capability to reduce the readout noise of an optical and X-ray photon detector based on the semiconductor DEPFET device below a level of only $0.3e^-$ ENC (equivalent noise charge). The readout method used is called "Repetitive Non Destructive Readout" (RNDR) and was realised by placing two single DEPFET-devices next to each other and by coupling their charge storing region by an additional gate. By transferring the stored charge from one DEPFET to the other and vice versa the same charge can be measured non-destructively and arbitrarily often. Taking the average value of a large number n of these measurements, the noise is reduced by $1/\sqrt{n}$. The main advantage of such a detector is to greatly reduce the influence of the $1/f$ noise to the readout noise. The theoretically and experimentally achievable resolution for different operating parameters (leakage current, readout noise, number and duration of readouts) was investigated by Monte-Carlo simulations and verified on a real RNDR minimatrix (pixelarray). Single optical photon detection with high quantum efficiency and, even more fascinating, the possibility to distinguish between different numbers of photons e.g. 100 from 101 is presented in measurements.**

***Index Terms*— single optical photon detection, RNDR, sub-electron noise, DEPFET, Active Pixel Sensor, low noise readout.**

I. Introduction

ONE of the most important questions of operating a semiconductor radiation device is how precise the amount of produced charge (electrons or holes) can be determined in a certain readout time given by the experimental constraints. Usually $1/f$ noise components limit the minimum achievable readout noise to a value not much smaller than $2e^-$ ENC, even for very long measurement times. By having the possibility to measure the amount of collected charge multiple times without loosing the charge during one readout, the uncertainty of many (n) of these measurements is reduced by $1/\sqrt{n}$ as explained in more detail later. In this work we demonstrate that a combination of two coupled DEPFET devices [1] fulfills the requirements for a repetitive non destructive readout. Also the concept can be used to build large radiation detector matrizes with homogenous entrance window and reasonable readout speed.

Manuscript received Nov 2006

S. Wölfel, S. Herrmann, M. Porro, L. Strüder and J. Treis are with the Max-Planck-Institut für extraterrestrische Physik, MPI Halbleiterlabor, Giessenbachstraße, D-85748 Garching, Germany (e-mail: steppke@hll.mpg.de).

R. H. Richter and G. Lutz are with the Max-Planck-Institut für Physik, MPI Halbleiterlabor, Föhringer Ring 6, D-80805 Munich, Germany.

P. Lechner is with PNSensor GmbH, Römerstraße 28, D-80803, Munich, Germany.

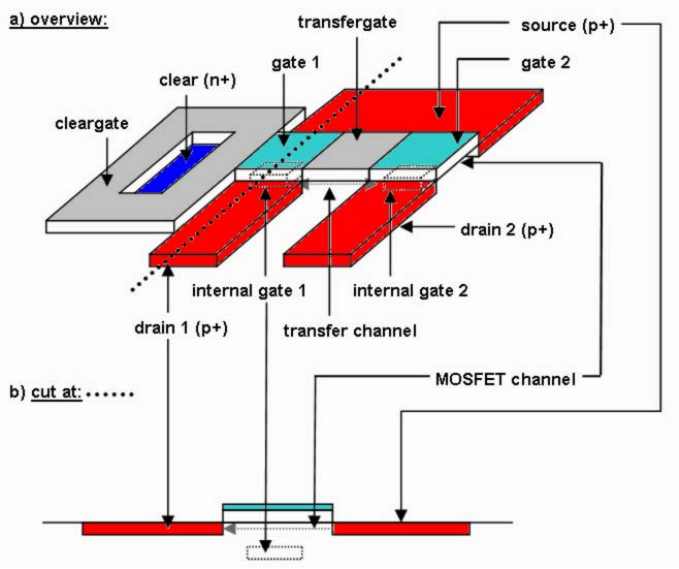

Fig. 1. Simplified layout of the investigated RNDR device. The collected charge is stored in the internal gates, located under the two external gates (**gate 1** and **gate 2**). The charge can drift from one DEPFET to the other by applying a positive voltage to the **transfergate**. The difference of the measured **source-drain** current of each transistor before and after a transfer is proportional to the transferred charge. Because the charge is not lost, but stored in the neighbouring DEPFET, its amount can be measured multiple times that way. The last transfer moves the charge under gate 1, from which it can be (now destructively) completely removed by opening the **cleargate** and applying a positive voltage to the **clear**.

Theoretical investigations on RNDR detectors have been carried out by Gatti et al. [2]. First measurements were shown by J. Janesick et al. with the floating gate based Skipper CCD, where noise values of $0.6e^-$ ENC have been published ([3] and [4]). The main difference in our approach is a reduction of the readout noise below the $0.3e^-$ ENC level, which is needed to separate single optical photons from the noise floor and also to distinguish between different numbers of single (photo-) electrons.

II. Device description

The essential attribute of a RNDR device [5] must be a complete signal charge storage during all readouts. The capability of a DEPFET-device [6] to store the collected signal electrons in a depleted region and to keep them isolated from other charge within the silicon bulk defines a feasible basic cell to build up a RNDR-device.

Our RNDR devices, which were designed and fabricated at the semiconductor laboratory (HLL) of the Max-Planck-Institutes for physics and for extraterrestrial physics in Munich, were realised by a combination of *two* DEPFET-devices and a transfergate between them which allows a controlled drift of signal charge from one DEPFET to the other (figure 1).

The DEPFET is a combined detector and amplifier structure, which consists of a p-channel-MOSFET processed on a high ohmic silicon substrate. Due to an implantation at the backside the bulk can be completely sideward depleted. This provides both, sensitivity over the whole wafer thickness as well as a lateral potential minimum for electrons beneath the wafer surface. Additional n-implanted regions beneath the two external gates of the MOSEFTs (gate 1 and gate 2, figure 1) force the generated (photo-) electrons to drift underneath the gates and confine them in an electric field. These locations are called "internal gates" [6]. The external gate of a DEPFET has two functions:

- As in a normal p-MOSFET the (hole-) current from source to drain is controlled by the applied gate-source voltage, so the DEPFET can be turned on and off by applying appropriate voltages to the external gate. A more negative gate-voltage increases the amount of mirror-holes in the transistor channel, and increases the source-drain current.
- If the external gate is turned off by applying a positive gate voltage the hole layer in the channel is removed and the internal gate becomes capacitively coupled to the external gate. A more positive external gate-off voltage makes the internal gate more attractive to electrons.

In the same way the external gate voltage controls the source drain current, the collected electrons in the internal gate also modulate the channel conductivity by creating mirror charges (holes) in the channel, and have therefore also an additional impact on the source-drain current (δI). The influence is described by $g_q = \frac{\delta I}{\delta Q}$ (δI: change in source-drain current, δQ: charge in the internal gate), according to $g_m = \frac{\partial I}{\partial V}$, the external gate transconductance. For our devices g_q is typically $\approx 300\frac{pA}{e^-}$. Because the DEPFET is charge collection point and first (integrated) amplifying stage at the same time, a small input capacitance of only a few tens of fF is achieved. This leads to a low noise and fast readout detector.

As seen in figure 1, the charge can be moved from the internal gate of the on-DEPFET, to the internal gate of the off-DEPFET, by applying a positive voltage to the transfergate, which acts as a n-channel MOSFET coupling the two internal gates. The essential part of the readout is measuring the current before and after transfer (indicated as thick red bars in figure 2, named b: measurement **b**efore and a: measurement **a**fter the transfer). The difference of the two measurements is δI (the process measurement - transfer - measurement is henceforth called one "readout"). The amount of moved charge (Q) can be derived from $Q = \frac{\delta I}{g_q}$ (fig. 2). By interchanging the on/off states of the two DEPFETs, the charge can be transferred back and measured again the same way. After repeating the measurement n times and taking the average value of all these measurements

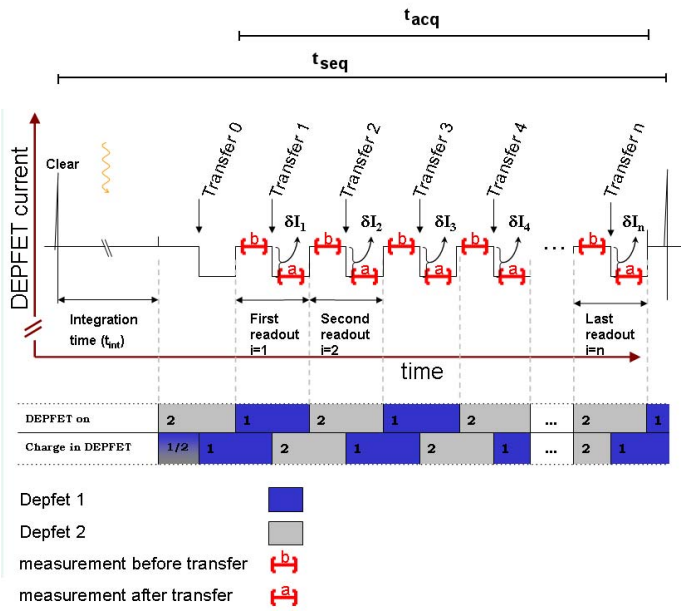

Fig. 2. This Plot shows the timing of one RNDR sequence. At $t = 0$ a clear removes all collected charges from the previous sequence. After that photoelectrons are collected and stored in the internal gates during the integration time t_{int}. The very first transfer (Transfer 0) moves all charges into the internal gate of DEPFET 1. After this the actual RNDR readout (t_{acq}) starts. For all n readouts the current is measured before (b) and after (a) each transfer. The differences of all these measurements ($\delta I_{i,i=1...n}$) is afterwards averaged, resulting in a reduces noise described by eq. 1.

the noise has decreased by statistics to

$$\sigma_{end} = \frac{\sqrt{\sigma_1^2 + \sigma_2^2 + \cdots + \sigma_n^2}}{n} = \frac{\sqrt{n \cdot \sigma^2}}{n} = \frac{\sigma}{\sqrt{n}}. \quad (1)$$

n	: number of readouts (e.g. number of transfers)
σ_i	: readout noise of measurement i
σ_{end}	: readout noise after n readouts
σ	: mean noise of one readout, $\sigma = \sigma_{i,i=1...n}$

After all n readouts of one sequence (t_{seq}), an additional n-channel-MOSFET (cleargate, figure 1) is opened and a positive voltage at the clear contact removes the charge. The internal gates of the two DEPFETs are now empty and ready for further charge collection.

The main advantage of this readout principle is that even if all single measurements are affected by 1/f noise, this shaping-time independent noise source is also reduced by eq. 1. Imagine a detector where the 1/f noise becomes dominant for effective measurement times longer than $20\mu s$. In this case it is better to measure the collected charge e.g. 5 times for $20\mu s$ each (and taking the average value) than measuring once for $100\mu s$. For these example numbers you can not win in noise reduction by measuring much longer than $20\mu s$, due to low frequency 1/f noise components.

The only noise limiting factor remaining is the leakage current rate (i_l). Every leakage current electron entering the internal gate during t_{acq} highers the number of collected

electrons by one. The influence of this effect to the achievable noise value is discussed in the following section.

III. Simulations

To understand the influence of the leakage current, which is not included in eq. 1 to the overall detector performance Monte-Carlo simulations have been carried out. Also a short evaluation of single optical-photon imaging is given.

A. Monte-Carlo

To investigate a RNDR device from the theoretical point of view the four most important parameters to be looked at are:

i_l	leakage current rate in $e^-/(\mu s \cdot\ pixel)$
t_{loop}	readout time for one readout in μs
σ	readout noise for one readout in e^- ENC
n	number of readouts

The influence of these values to the achievable resolution was investigated by Monte Carlo simulations. The mean value $x_{k(k=1...q)}$ of all n readouts is calculated from eq. 2:

$$x_{k(k=1...q)} = \frac{\sum_{i=1}^{n} (p_i \pm \sigma)}{n} \tag{2}$$

whereas

n	number of readouts
q	overall Monte-Carlo runs
k	number of Monte-Carlo run, $k = 1...q$
x_k	mean value of all readouts of one Monte Carlo run
p_i	number of collected electrons till readout number i
$\pm\sigma$	indicates, that p_i is affected by gaussian distributed noise with a variance of σ

Also important for the discussion is the integration time t_{int} which is the time from last clear up to the beginning of the readout (fig. 2). The distribution of the number of leakage current electrons for an infinite ($q \rightarrow \infty$) number of Monte Carlo runs corresponds to the poisson distribution for the given leakage current rate i_l and the acquisition time $t_{acq} = n \cdot t_{loop}$.

B. Influence of the leakage current

The Monte Carlo simulation generates the randomly distributed arrival times of the leakage current electrons according to the leakage current rate i_l. Fig. 5 presents an overview of the probability to get a certain number of leakage current electrons for a given mean amount of electrons (during t_acq). Let us assume a leakage current electron reaching the detector during the acquisition time while readout number i is performed. Thus the number of collected electrons p_i is increased by one for all following readouts. The amount of increase of x_k produced by this depends on the arrival time of the charge. An electron entering the detector at the end of the acquisition time (i high according to n) is weighted less than an electron arriving close to the beginning (i low according to n). Running the simulation q times for a given leakage current of $0.00002e^-/(\mu s \cdot pixel)$, but different number of readouts with adding serial noise of

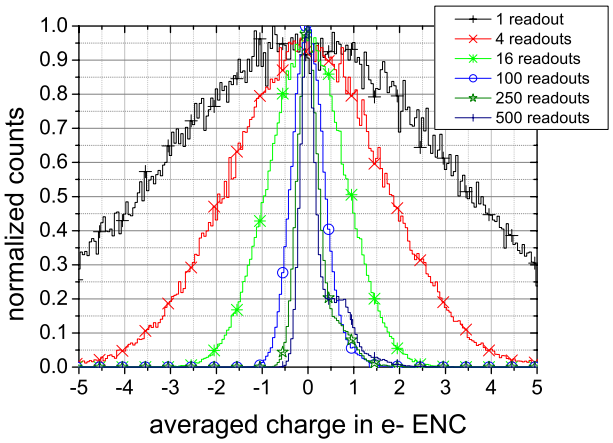

Fig. 3. Simulated noisepeaks of a RNDR detector with $\sigma = 3.3e^-$ ENC for different numbers of readouts n for a given leakage current of $i_l = 0.00002e^-/(\mu s \cdot Pixel)$ and a time for one readout of $t_{loop} = 51\mu s$. The noise decreases with increasing number of readouts up $n \approx 360$ readouts. It becomes worse for higher number of readouts, because of the leakage current influence.

$\sigma = 3.3e^-$ to every readout's value produces noise peaks whose widths become smaller with increasing number of readouts for n up to ≈ 360 (fig. 3), because the noise is reduced by eq. 1. For longer acquisition times ($n > 360$) the noisepeaks become asymmetric with tails to higher values, because the positions and shapes are now determined by the leakage current mainly (fig. 4).

The isolines of fig. 6 show the standard deviation of the noise peak for variable values for leakage current rate i_l and number of readouts n, with a fixed readout noise of $\sigma = 3.3e^-$ ENC and readout time $t_{loop} = 51\mu s$. This plot depicts, that for a given leakage current an optimum number of readouts n exists, were the lowest noise value can be achieved.

C. Discussion of the noise level

If later used as a RNDR-based imaging matrix device, it is important to unterstand, what a certain resolution means in terms of contrast. To get an idea of this a simulated 30 by 30 RNDR-pixel matrix was filled with one electron in each pixel position marked in the first plot of figure 7 in black (mask, no noise). Afterwards gaussian distributed noise with $\sigma = 1, 0.5, 0.3, 0.2$ and $0.1e^-$ ENC was added to each matrix-pixel. The plots show, that a resolution of better than $0.3e^-$ ENC is required to separate a one electron (photon) structure from the noise.

IV. Experimental results

To verify the theoretical model, measurements on different devices have been done. To reduce the influence of the leakage current, the measurement setup, consisting of the RNDR device itself, bonded to a ceramic carrier, and the first amplifying

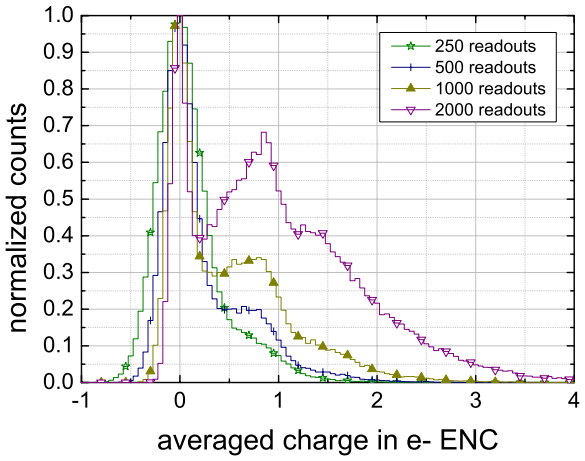

Fig. 4. Same simulation as shown in fig. 3 but for higher numbers of readouts ($n = 250, 500, 1000$ and 2000). The influence of the leakage current can be seen by the shift to higher values. But because the leakage current rate is quite low, it is still possible that for some sequences no leakage current electrons enter the RNDR-device, resulting in events found in the very narrow part of the noise peak positioned around $0e^-$.

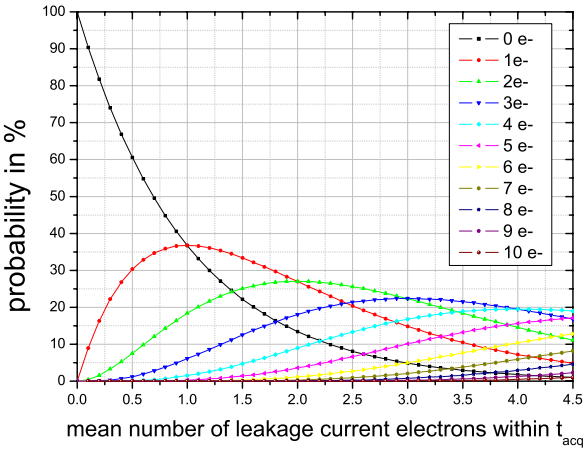

Fig. 5. Poisson calculated probability to get a certain number of leakage current electrons for different number of mean leakage current electron values.

readout electronic was operated in a climatic chamber at temperatures down to $-55°C$.

A. Setup

Figure 8 shows a simplified scheme of the readout setup. The two DEPFETs, on which our RNDR device are based on, have one common Source and two individual drains (figure 1), which are connected together to one readout node. The amplifier provides the virtual drain potential $V_{virtual\ drain}$. The current change due to electrons in the internal gate is small compared to the baseline current flowing through the DEPFET in the on-state. This baseline current can be subtracted by choosing a proper value of $V_{subtr.}$. The amplification is done via an I/V (current-to-voltage) converter as a first stage and a voltage amplifier as a second stage (not shown in figure 8). A main sequencer (FPGA) controls the voltages for the external gates, transfergate, cleargate and clear, and triggers the ADC (analog to digital converter) to sample the amplified output current of the device.

B. Noise measurements

To verify the simulated data, measurements were done by investigating one pixel of a 4 by 4 RNDR minimatrix. In figure 9 the measured noise is shown for a variation of the readout numbers from $n = 2$ to $n = 200$ for three different temperatures of $-30°C$ (purple), $-40°C$ (red) and $-55°C$ (black). As can be seen, the decrease in noise follows the $1/\sqrt{n}$ law (blue) up to a certain number of readouts, which depends on the temperature (e.g. $n_{best} \approx 100$ for the $-30°C$ measurement). Figure 10 shows the same plot for a higher

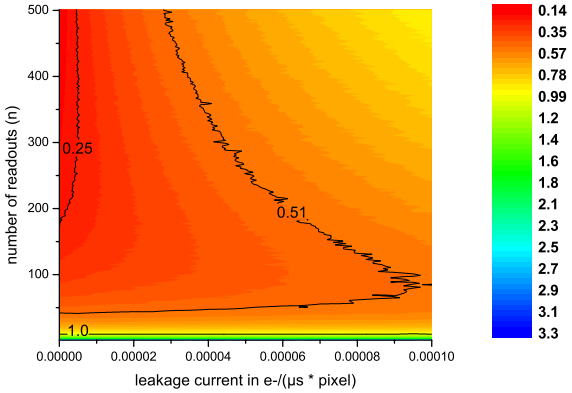

Fig. 6. Monte-Carlo simulated map showing the achievable noise in e^- colorcoded for a variation of the leakage current and the number of readouts. It can be seen, that for a given leakage current an optimum number of readouts n exists, were the best noise σ_{end} can be achieved. Simulation parameters: $\sigma = 3.3e^-$ ENC, $t_{loop} = 51\mu s$. To see the pure impact of the leakage current to the resolution an integration time of only $t_{int} = 1\mu s$ was used

number of readouts of up to $n = 2000$, which corresponds to an acquisition time of $t_{acq} = 51ms$. The degradation of the readout noise shown here can be explained by the higher probability that a leakage current electron enters one of the two internal gates during acquisition time (as theoretically investigated in III-B).

The mean leakage current in the case of the $-55°C$ measurement with $n = 2000$ readouts was $0.98\frac{e-}{t_{acq}}$, resulting in a probability of 37% that no leakage electrons enters the detector during the 2000 readouts, 36% that one electron enters the detector, 18% that two electrons enter the detector and 9% that

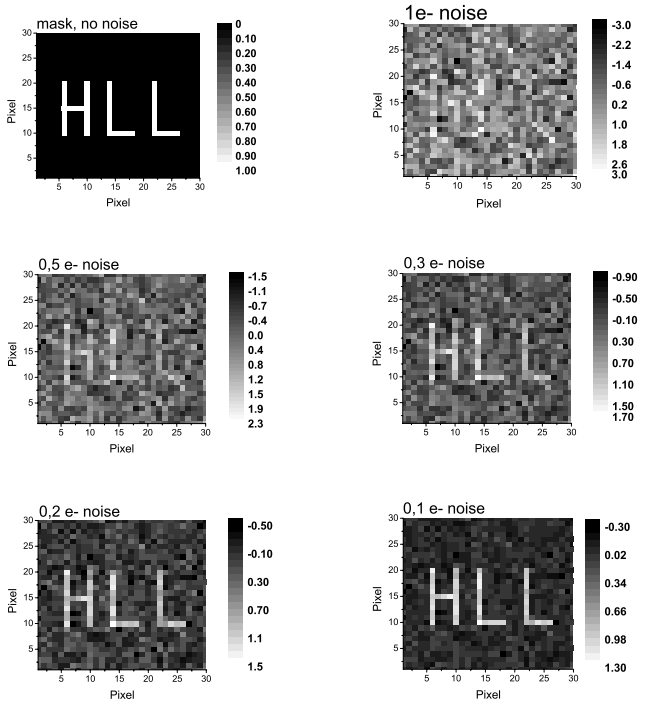

Fig. 7. These six plots show simulated maps for different noise levels ($0, 1, 0.5, 0.3, 0.2$ and $0.1e^-$ ENC). The pixels shown in plot number one (image mask) in black are filled with one additional signal electron (photon). At a present noise level of better than $0.3e^-$, the mask-structure becomes clearly separable from the background.

three or more electrons enter during the readouts (fig. 5). These in time randomly distributed leakage current electrons broaden the noise peak and shift it also to higher values.

C. Single photon spectra

To test the detector under optical photon illumination working parameters of $T = -45°C$, $n = 360$ and $t_{loop} = 25\mu s$ have been chosen. All readout sequences k started with a clear and followed by a short photon injection with a weak laser source (672 nm) during t_{int}. Afterwards the amount of collected photoelectrons was measured $n = 360$ times, the average value x_k taken and this value arranged in a histogram which is shown in figure 11 for a very weak laser intensity and in figure 12 for a higher laser intensity, were the mean number of collected photoelectrons was e.g. in this measurement twelve. The peaks belonging to different numbers of electrons can clearly be distinguished. Also the quantum poisson nature of the laser source can be nicely seen in the two plots. In the case of fig. 12 the poisson statistics can be approximated by a gaussian distribution fitted by the envelope curve with a width of $3.48 \approx \sqrt{12}$. An experimental example of the influence of the leakage current to the noise peak (cap. III-B) can be found in figure 11 by the asymmetric noise peak (black). A description of the noise peak with only one parameter (e.g. σ) is not exhaustive here.

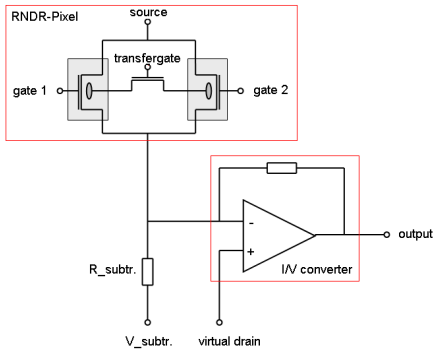

Fig. 8. Simplified scheme of the RNDR device and the readout setup. The current-to-voltage (I/V) converter defines a common drain potential for both DEPFETs ($V_{virtual\ drain}$). By turning one DEPFET off during the other one is on and vice versa enables the readout of both DEPFETs with only one readout node.

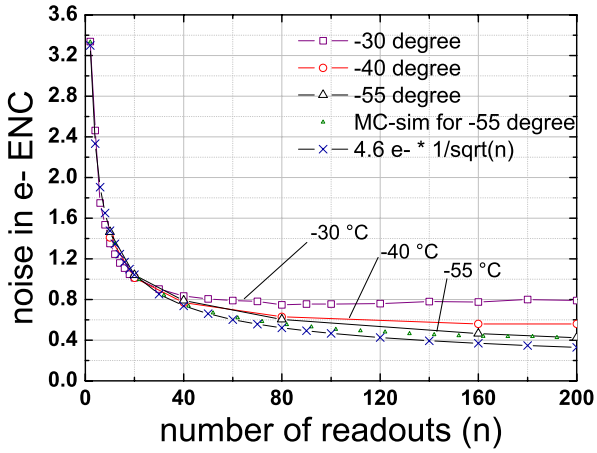

Fig. 9. Measured noise in e^- ENC vs number of readouts. To get a concise plot, the first measurement point shown is already the mean value from two readouts ($n = 2$ $\sigma_{end} = 3.3e^- ENC$). For three different temperatures of $-30°C$, $-40°C$ and $-55°C$ measurements are shown, the monotonously falling blue curve shows the respective theoretical noise limit given by eq. 1

Figure 13 was obtained by a stepwise increase of the laser intensity from 0 to approximately 130 collected photoelectrons and by adding all results in one histogram. It shows nicely that the readout mechanism behaves linear also for a higher amount of collected electrons, and that calibration can be done by simply counting the peaks. Figure 14 shows the highlighted area of fig. 13 magnified. It displays in more detail that e.g. 100 electrons can be be clearly distinguished from 101.

V. Outlook and Applications

Although the results were very promising so far there is still space for future improvements. A further reduction in readout noise is expected by

- using a faster acquisition system with integrated ASIC and

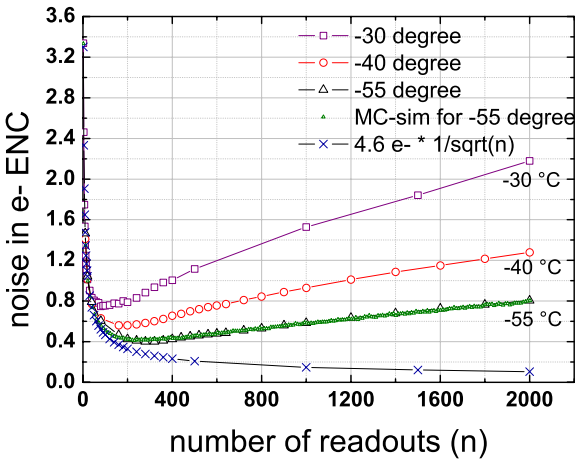

Fig. 10. Same measurement as shown in figure 9, but for up to $n = 2000$ readouts. Due to a longer measurement time the leakage current limits the maximum achievable resolution. Because the leakage current is smaller for colder temperatures the best value was achieved at $-55°C$.

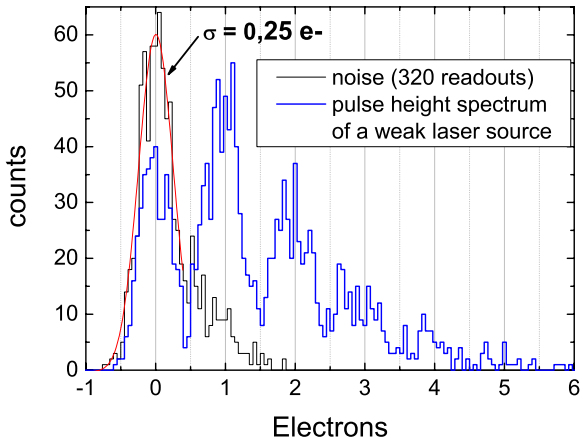

Fig. 11. Single electron pulse height spectrum obtained by injection of photoelectron during t_{int} with a weak laser source. One readout was done with a precision of $\sigma = 4.6e^-$. A fit over the gaussian part of the noise peak (leakage current influence is unattended) results in a resolution of only $\sigma_{end} = 0,25e^- \approx \frac{4.6e^-}{\sqrt{360}}$

a faster gate- and transfergate switcher which will shorten t_{acq} and thus reduce the influence of the leakage current.

- cooling down to $-80°C$ and less will further reduce the leakage current.
- reducing the readout noise σ of one readout to values down to $2e^-$ ENC and less, as was shown for DEPFET detectors with smaller gatelength, will help to reduce the number of readouts n needed to achieve a certain resolution. Such devices are currently under production.

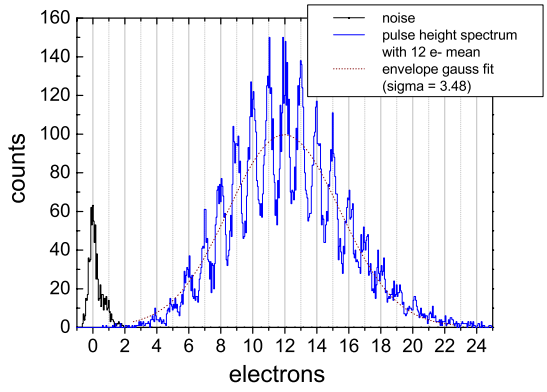

Fig. 12. Single electron spectrum obtained the same way than fig. 11 but with a mean photoelectron injection of here 12 electrons. The poisson distributed quantum nature of the laser source used can be nicely seen by the gaussian fit with a width of $\approx \sqrt{12}$.

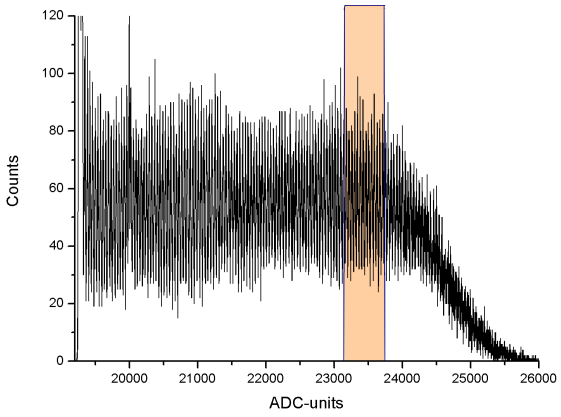

Fig. 13. Histogram obtained by a stepwise increase of the laser intensity and adding all results to one histogram. This way, the calibration of a RNDR detector can be done by simply counting the peaks.

The most obvious application of such a detector is single optical photon detection in low flux environments, for example in the field of astronomy, where faint galaxies or stars shall be characterized even though only a extremely low number of emitted photons reaches the earth.

Another auspicious research field is molecular biology. Here the detection of a few photons emitted by only a small number optical fluorescence tracer molecules, which had been attached to molecules under research, is needed to learn more about the reaction behavior of such molecules.

But because of the detector's ability to dynamically adapt a desired resolution by choosing a proper number of readouts, also a low noise X-ray detector can be realised by measuring the charge e.g. only 4 times to end with a resolution two times better than the resolution of one readout. By this means a resolution of $1e^-$ ENC ($\sigma = 2e^- ENC$) can be achieved which

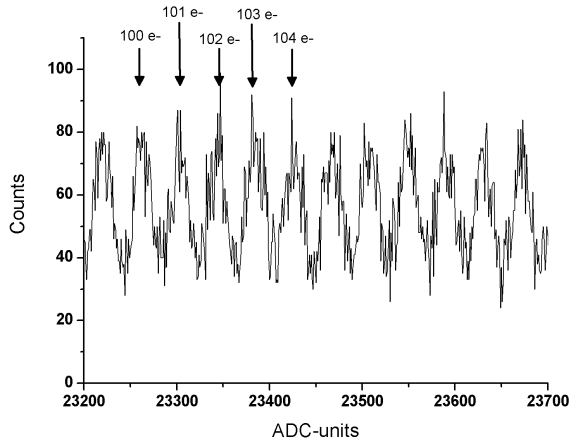

Fig. 14. Zoom in fig. 13. Even 100 collected photoelectrons can clearly be distinguished from $101, 102, 103$ and so on.

leads to a 5 σ X-ray noise cut at 18.2 eV. Of course the entrance window of the detector must be able to handle such photons, but this resolution would allow to see e.g. Iron or Carbon lines from far away extremely red-shifted astronomical X-ray objects.

VI. Conclusion

It was theoretically and experimentally shown, that with our DEPFET-based RNDR-detector a noise value down to $0.25e^-$ ENC can be achieved by using the method of repetitive non-destructive readout. To our knowledge this is the lowest readout noise value ever measured with linear amplifying detectors. It has been shown that the DEPFET is very appropriate to fulfill the requirements to realize such a readout element. The produced single pixels and minimatrix prototypes show promising results at moderate cooling of only $-55°C$. Because matrix operation is also possible with DEPFETs, larger area sensors are currently under production, to obtain position sensitive single photon detection. Another promising approach is, using a single RNDR-device as a readout node for a CCD column. Such devices are also under production and combine the good CCD properties with a ultra low noise readout.

References

[1] J. Kemmer and G. Lutz, "New detector concepts," *Nucl. Instr. and Meth. A*, vol. 253, p. 356, 1987.

[2] E. Gatti, A. Geraci, and C. Guazzoni, "Multiple read-out of signals in presence of arbitrary noise optimum filters," *Nucl. Instr. and Meth. A*, vol. 417, p. 342, 1998.

[3] J. Janesick, T. Elliott, A. Digizian, R. Bredthauer, C. Chandler, J. Westphal, and J. Gunn, "New advancements in charge-coupled device technology - subelectron noise and 4096x4096 pixel ccds," *Astronom. Society of Pacif. Conf.*, vol. Series No. 6, 1989.

[4] R. Kraft, D. Burrows, G.P.Garmire, J.A.Nousek, J. Janesick, and P. Vu, "Soft x-ray spectroscopy with sub-electron readnoise charge-coupled devices," *Nucl. Instr. and Meth. A*, vol. 361, p. 372, 1995.

[5] S. Wölfel, S. Herrmann, P. Lechner, G. Lutz, M. Porro, R. Richter, L. Strüder, and J. Treis, "Sub-electron noise measurements on repetitive non-destructive readout devices," *Nucl. Instr. Meth. A 566 (2006) 536-539*, vol. 566, pp. 536–539, 2006.

[6] J. Treis, P. Fischer, O. Haelker, M. Harter, S. Herrmann, R. Kohrs, H. Krueger, P. Lechner, G. Lutz, I. Peric, M. Porro, R. H. Richter, L. Strueder, M. Trimpl, and N. Wermes, "Depmosfet active pixel sensor prototypes for the xeus wide field imager," *IEEE-TNS*, vol. 52, No. 4, p. 1083, 2005.